CIRCULAR DOOR KNOCKER STRIKING PLATE - CU ALLOY - MODERN TIMES - SWITZERLAND

Artefact name	Circular door knocker striking plate
Authors	Marianne. Senn (Empa, Dübendorf, Zurich, Switzerland) & Christian. Degrigny (HE-Arc CR, Neuchâtel, Neuchâtel, Switzerland)
Url	/artefacts/919/

The object

Credit HE-Arc CR.

Fig. 1: Circular door knocker striking plate (after Benoît, 1994),

Description and visual observation

Description of the artefact	Circular striking plate no 2 (from a set of two) of a door knocker with a protruding lion head holding a hinge in his fangs, Ø.ext = 64cm. The circular base is said to be covered by a gilded decorative relief (Fig. 1, Benoit, 1994, 6).
Type of artefact	Architectural element
Origin	Door knocker of Lausanne cathedral, Lausanne, Vaud, Switzerland
Recovering date	Unknown
Chronology category	Modern Times

chronology tpq	1601 A.D.
chronology taq	1700 A.D.
Chronology comment	17th Century AD
Burial conditions / environment	Outdoor atmosphere
Artefact location	Lausanne cathedral, Lausanne, Vaud
Owner	Lausanne cathedral, Lausanne, Vaud
Inv. number	None
Recorded conservation data	N/A

Complementary information

None.

Study area(s)

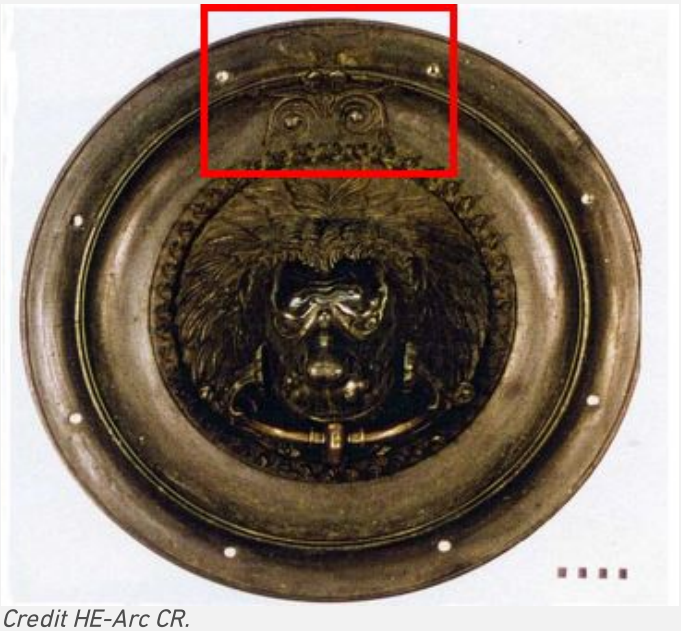

Credit HE-Arc CR.

Fig. 2: Possible location of sampling area,

Binocular observation and representation of the corrosion structure

None.

MiCorr stratigraphy(ies) – Bi

Sample(s)

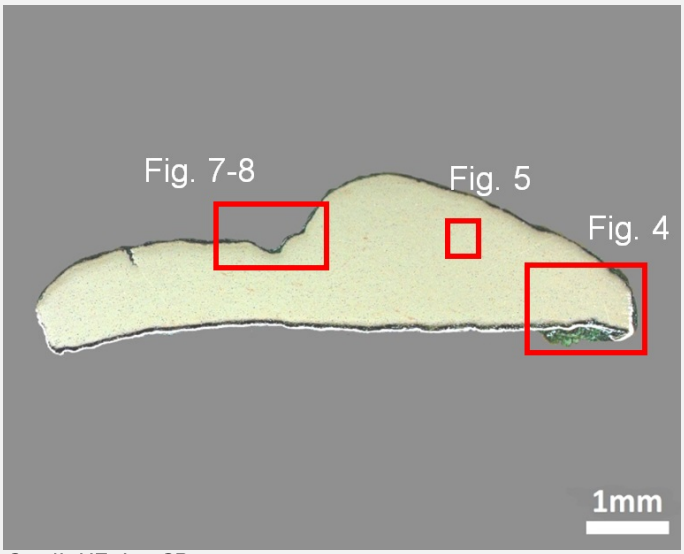

Fig. 3: Micrograph of the cross-section of the sample taken from the circular plate showing the location of Figs. 4 to 5 and 7 to 8,

Credit HE-Arc CR.

Description of sample	No information is given on where the sample has been taken. A supposed location is however illustrated in Fig. 2. The polished sample shows a well preserved metal surface with some cracks covered by a thin corrosion crust (Fig. 3).
Alloy	Cu Alloy
Technology	Rolled, annealed after cold working
Lab number of sample	MAH 94-156-001
Sample location	Musées d'art et d'histoire, Genève, Geneva
Responsible institution	Musées d'art et d'histoire, Genève, Geneva
Date and aim of sampling	1994, metallography and presence or not of a gilding treatment

Complementary information

None.

Analyses and results

Analyses performed:
Metallography (etched with ferric chloride reagent), Vickers hardness testing, LA-ICP-MS, SEM/EDS, Raman spectroscopy.

Non invasive analysis

None.

Metal

Analysis by LA-ICP-MS (Table 1) indicates that the metal is a copper-rich alloy. The high relative standard deviations (RSD) result from the heterogeneity of the metal (inclusions). The alloy differs from the quaternary alloy given in the report for the circular base considered here (Benoît 1994, p.18). It contains numerous inclusions of copper oxides (Figs. 4, 5, 7 and 8, Table 2) and heavy metals (Sn, Pb, Fig. 8 and Table 2) that are residues from the manufacturing process. In polarized light, the copper oxide inclusions appear red (Figs. 4 and 7) while with SEM in BSE-mode they look light-grey (Fig. 8). Heavy metals inclusions appear white with SEM (BSE-mode, Fig. 8). Due to the rolling process the copper oxide inclusions are parallel to the longitudinal orientation of the sample (Figs. 4 and 5). They were identified as cuprite by Raman spectroscopy (Fig. 6). The etched alloy shows a structure of polygonal grains with annealing twins (Fig. 5). The grain size is variable. The average hardness of the alloy is HV1 80, which is quite high compared to the average hardness of a pure annealed copper of around HV1 40-50 (Schumann 1991, 627).

Elements	Cu	Sb	Pb	Ag	Bi	Sn	Zn	Ni	As	S
mass%	99.6	0.2	0.12	0.1	0.004	<	<	<	<	<
RSD %	0.3	112	132	1	112					

Table 1: Chemical composition of the metal. Method of analysis: LA-ICP-MS, Laboratory of Basic Aspects of Analytical Chemistry at the Faculty of Chemistry, University of Warsaw, PL.

Elements	O	Cu	Fe	Ni	Sn	Sb	Pb	Total
Light-grey inclusion	10	86	<	<	<	<	<	96
White inclusion 1	18	48	17	3	11	0.9	0.8	105
White inclusion 2	13	8	<	<	<	34	44	99

Table 2: Chemical composition (mass %) of the inclusions (light-grey and white in Fig. 8) in the metal. Method of analysis: SEM/EDS, Laboratory of Analytical Chemistry, Empa.

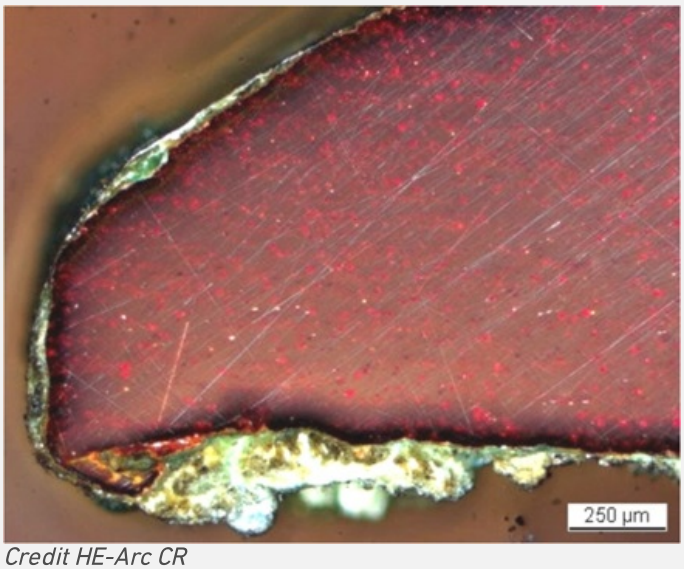

Credit HE-Arc CR

Fig. 4: Micrograph of the metal sample from Fig. 3 (reversed picture), unetched, polarised light. The red copper oxide inclusions form rows in the copper alloy matrix,

Fig. 5: Micrograph of the metal sample from Fig. 3 (detail), etched, bright field. The metal shows a structure of polygonal and twinned grains. Copper oxide inclusions are visible as dark spots,

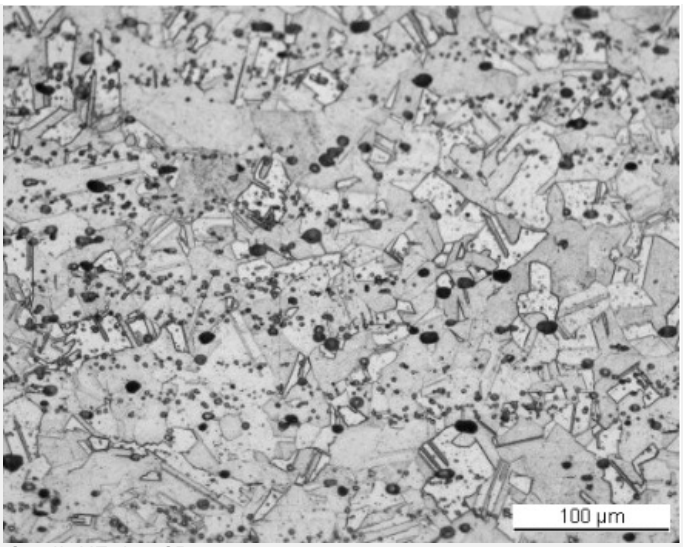

Credit HE-Arc CR.

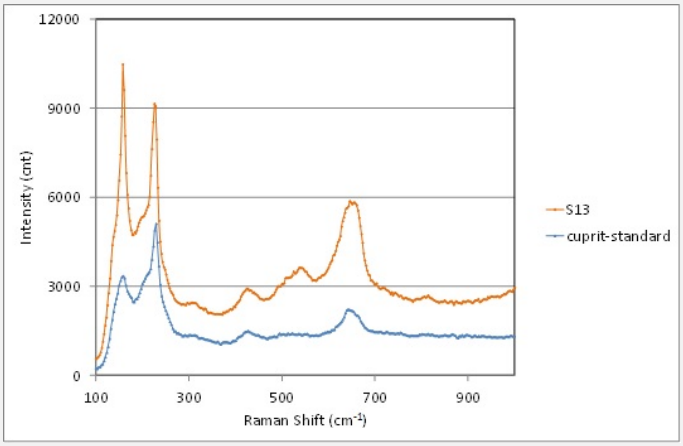

Credit SNM.

Fig. 6: Raman spectrum of a red inclusion (S13) of Fig. 4 compared to a cuprite standard spectrum. Settings: laser wavelength 532nm, acquisition time 100s, one accumulation, filter D2 (0.75-0.8mW), hole 500, slit 80, grating 600. Method of analysis: Raman spectroscopy. Lab of Swiss National Museum, Affoltern a. Albis ZH,

Microstructure	Polygonal and twinned grains, elongated inclusions
First metal element	Cu
Other metal elements	Ag, Sb, Pb

Complementary information

None.

Corrosion layers

The average thickness of the corrosion crust is about 90µm, but may be thinner or thicker depending on the area of origin (Fig. 4). Under polarized light, we observe a multilayer system with a dense and thin inner red corrosion layer (CP2, probably cuprite/Cu2O) on the metal (Fig. 7) containing chlorides (Fig. 8 and Table 3). This is followed by bands of heterogeneous green corrosion products (CP1, possibly copper chloride / sulphate / carbonate). This outer corrosion layer is contaminated with atmospheric components (Si, Al, Cl, C and O and perhaps gypsum particles (CaSO4)) (Fig. 8).

Elements	O	Si	Cl	Cu	Total
CP2, inner red layer	11	<	23	60	94

Table 3: Chemical composition (mass %) of the inner corrosion layer (CP2). Method of analysis: SEM/EDS, Laboratory of Analytical Chemistry, Empa.

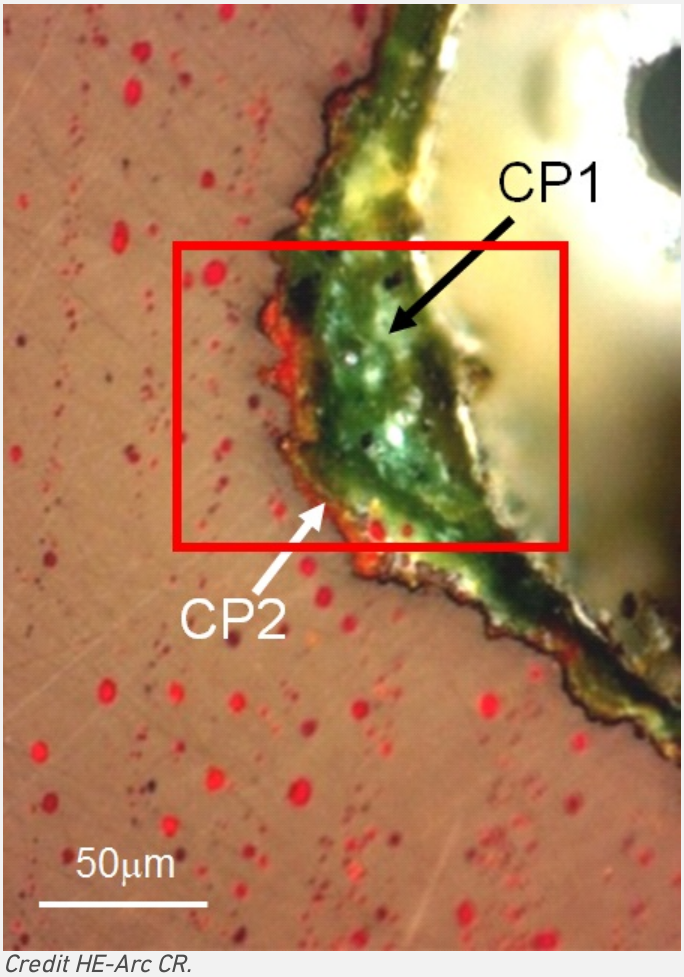

Credit HE-Arc CR.

Fig. 7: Micrograph of the metal sample from Fig. 3 (rotated by 90°) and corresponding to the stratigraphy of Fig. 9, polarised light. Metal with red copper oxide inclusions. The black particles in the green corrosion layer are quartz inclusions. The area selected for elemental chemical distribution (Fig. 8) is marked by a red rectangle,

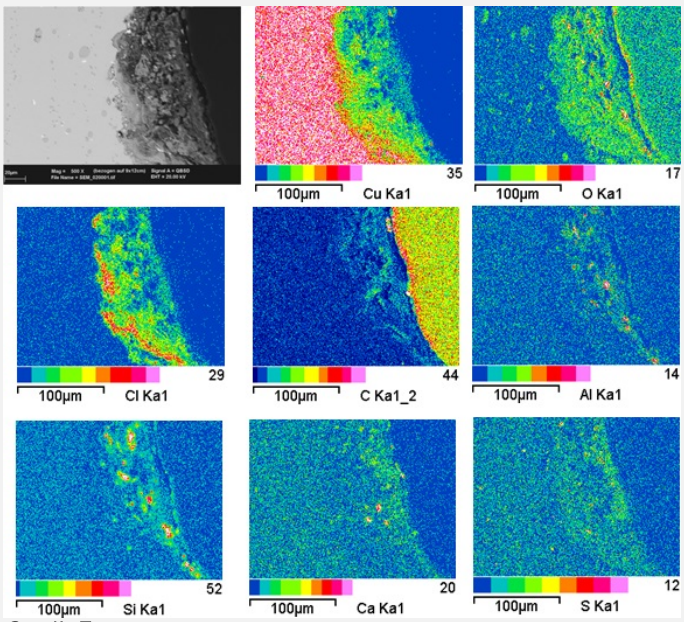

Credit Empa.

Fig. 8: SEM image, BSE-mode, and elemental chemical distribution of the selected area of Fig. 7. Method of examination: SEM/EDS, Laboratory of Analytical Chemistry, Empa,

Corrosion form	Uniform - pitting
Corrosion type	Mostly type I with locally type II (Robbiola)

Complementary information

None.

MiCorr stratigraphy(ies) – CS

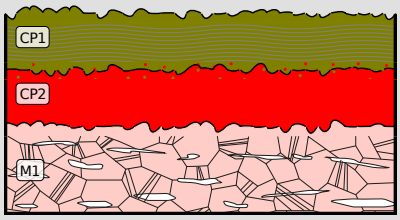

Fig. 9: Stratigraphic representation of the sample taken from the circular base in cross-section (dark field) using the MiCorr application. The characteristics of the strata are only accessible by clicking on the drawing that redirects you to the search tool by stratigraphy representation. This representation can be compared to Fig. 7, Credit HE-Arc CR.

Synthesis of the binocular / cross-section examination of the corrosion structure

None.

Conclusion

The circular striking plate of the door knocker consists of a rolled copper alloy that was annealed after cold working. The metal is rich in copper oxide inclusions. The corrosion is most likely composed of cuprite in proximity to the metal surface, followed by green copper corrosion products (possibly chlorides, carbonates or sulphates) on the outer surface which is also contaminated with gypsum and airborne particles. The presence of chlorides in the inner corrosion layers could be explained by contamination through handling. Soil elements are probably originating from airborne dust, whereas sulphur could come from urban SO2 pollution. No trace of gilding was observed. In this case the corrosion is mostly of type 1, but can be locally of type 2 after Robbiola et al. 1998.

References

References on object and sample

1. Benoît, C. (1994) Cathédrale de Lausanne: conservation de deux appliques en bronze à tête de lion avec anneau mobile et encadrement circulaire. Rapport de travail, non publié.
2. Rapport d'examen (1998) Laboratoire Musées d'Art et d'Histoire, Genève No 94-156-1/2.

References on analytic methods and interpretation

3. Robbiola, L., Blengino, J-M., Fiaud, C. (1998) Morphology and mechanisms of formation of natural patinas on archaeological Cu-Sn alloys, Corrosion Science, 40, 12, 2083-2111.
4. Schumann, H. (1991) Metallographie, Leipzig.